Nr 2 (73–140) LUTY 2024 Tom LXIX

POLIMERY

Influence of the ester block polymerization degree on the structure and properties of ester-ether-amide block terpolymers

Joanna Rokicka[1), *)] (ORCID ID: 0000-0002-2003-6372), **Jolanta Janik**[1)] (0000-0002-8094-8509), **Beata Schmidt**[1)] (0000-0001-6274-2278), **Katarzyna Wilpiszewska**[1)] (0000-0003-2756-3471)

DOI: https://doi.org/10.14314/polimery.2024.2.1

Abstract: New multi-block thermoplastic elastomers (TPEEA) were obtained, consisting of a crystalline amide block (domains), an amorphous ether block (continuous phase) and an ester block with a variable degree of polymerization, which acts as a compatibilizer. The presence of large interfacial areas was observed. It was found that ester blocks with a molecular weight <600 g/mol mix with other blocks, modifying the phases that constitute them and stabilizing the micro- and nanophase structure of the entire system. Short ester blocks act as nucleation precursors, and in the hard phase they have plasticizing properties.

Keywords: thermoplastic elastomers, phase structure, block copolymers.

Wpływ stopnia polimeryzacji bloku estrowego na strukturę oraz właściwości blokowych terpolimerów estrowo-eterowo-amidowych

Streszczenie: Otrzymano nowe wieloblokowe elastomery termoplastyczne (TPEEA), składające się z krystalicznego bloku amidowego (domeny), amorficznego bloku eterowego (faza ciągła) oraz bloku estrowego o zmiennym stopniu polimeryzacji, który pełni funkcję kompatybilizatora. Zaobserwowano obecność dużych obszarów międzyfazowych. Stwierdzono, że bloki estrowe o masie cząsteczkowej <600 g/mol mieszają się z innymi blokami, modyfikując tworzące je fazy i stabilizując strukturę mikro- i nanofazową całego układu. Krótkie bloki estrowe pełnią funkcję prekursorów zarodkowania, a w fazie twardej mają właściwości uplastyczniające.

Słowa kluczowe: elastomery termoplastyczne, struktura fazowa, kopolimery blokowe.

Thermoplastic elastomers (TPEs) exhibit the flexibility of traditional elastomers with the ease of processing and recycling, characteristic for thermoplastics [1–5]. Essential is the occurrence of thermally reversible physical crosslinking. The decomposition of the network nodes at high temperatures and their reconstitution while cooling enables these materials to repeatedly transition from a glassy or semicrystalline solid state to a viscous liquid [6–8]. Thus, the TPE network can exist up to a temperature determined by the forces of intermolecular interactions. Below this temperature, and above the glass transition temperature, such a polymer exhibits the characteristics of a chemically cross-linked rubber. The synthesis of TPE can be considered as forming the thermo-reversible network nodes, which are stable

[1)] Department of Organic Chemical Technology and Polymer Materials, Faculty of Chemical Technology and Engineering, West Pomeranian University of Technology in Szczecin, al. Piastów 17, 70-310 Szczecin, Poland.

[*)] Author for correspondence: joanna.rokicka@zut.edu.pl

during the product application, and decomposing without degradation at a temperature of TPEs processing [9].

Conventional TPEs are heterophase systems in which at least two immiscible phases coexist: a soft and a hard state, which are mutually dispersed or chemically bonded [10–15]. The soft phase is a continuous matrix and is responsible for the elasticity. The domains of the hard phase are dispersed in a matrix and are responsible for the strength and processing properties of the material. Phase separation can occur when the result of the multiplication of the Flory-Huggins interaction parameter χ by the degree of polymerization N exceeds a critical value [16]. Thus, by increasing the degree of polymerization of flexible or rigid segments, it is possible to induce phase separation (already initiated in the polymer melt during polymerization, the so-called melt phasing) [17–19]. The part of the rigid segments that do not undergo phase separation remains dissolved in the soft phase, leading to an increase in the glass transition temperature of this phase. The phase-separated rigid segments have two functions: the physical cross-linking agent (network nodes) and the filler (reinforcement) [20–22].

The properties of TPEs are the result of a combination of blocks' characteristics, thus essential in the materials design is to select the parts of the system that allow a stable micro- or nanostructure to be formed. Presently, the most used TPE flexible blocks are PEG [23–27], PTMO [28–33], and polyetheramine [34–36], as providing good flexibility and distribution of rigid block domains. The hard phase consists of amide blocks, including PA6 [37], PA11 [38, 39], and PA12 [40–42], that provide strong interactions within the domains and high mechanical strength.

The functional and processing properties of TPEs depend significantly on their physical structure and, in consequence, on the key factors, such as the individual blocks' content and chemical structure, molecular weight, and miscibility. In the recent reports, the two-block systems are comprehensively described. Their nanostructure and its effect on the copolymer properties are well known, and further research was focused on designing the new materials [43–46]. However, there are still relatively few publications on three-component systems. Introducing the third component into the diblock copolymer macromolecule affects the physical structure of the copolymer and the analysis of such systems is significantly complicated [47–51]. Therefore, in this work, new three-component TPEs were synthesized, and the physical structure and phase composition of these copolymers were discussed.

EXPERIMENTAL PART

Materials

For TPEEA synthesis, dimethyl terephthalate (DMT) (Elana, Poland); 1,3-propanediol (3G) (Sigma-Aldrich, USA); poly(tetramethyleneoxide)diol (PTMO) (M_w = 1000 g/mol, Du Pont, USA); α,ω-dicarboxilic oligo(laurolactam) (OA12) (M_w = 2000 g/mol) obtained in-house, according to the procedure described in [52]; pentaerythritol (technological additive increasing the melt viscosity of the polymer) – Brenntag, Germany; TiO_2/SiO_2 as a catalyst (Sachtleben Chemic GmbH, Germany); Irganox 1010 and Irgafos 126 as thermal stabilizers (Ciba Geigy, Switzerland); triethyl phosphate (TEP) as thermo-oxidative stabilizer (Rhodia, Belgium) were used.

For the OA12 synthesis, dodecano-12-lactam (Sigma-Aldrich, USA); sebacic acid (KSB) (Sigma-Aldrich, USA) and o-phosphoric acid (ChemPur, Poland), were used.

All raw materials used had a purity exceeding 99%.

Synthesis

The synthesis of oligoamide blocks terminated with carboxyl groups occurred in two stages. The first stage was performed under increased pressure (15 bar, 320°C, 5 h) in the presence of a molecular weight regulator (KSB), when the second stage involved polycondensation under atmospheric pressure (290°C, 5 h). To confirm the suitability of OA12 for further synthesis, its basic properties were characterized: the concentration of carboxyl groups, the concentration of amino groups and the melting temperature. The synthesis and characterization of oligoamides are described in detail in the previous work [52].

The synthesis of multi-block thermoplastic elastomers was carried out using a cascade of two reactors, which included: an ester exchange reactor (upper part) with a capacity of 3.6 dm^3 made of acid-resistant steel equipped with a dephlegmator and a cooler, a nitrogen dosing system, a heating system and an anchor mixer, and a polycondensation reactor (lower part) with a capac-

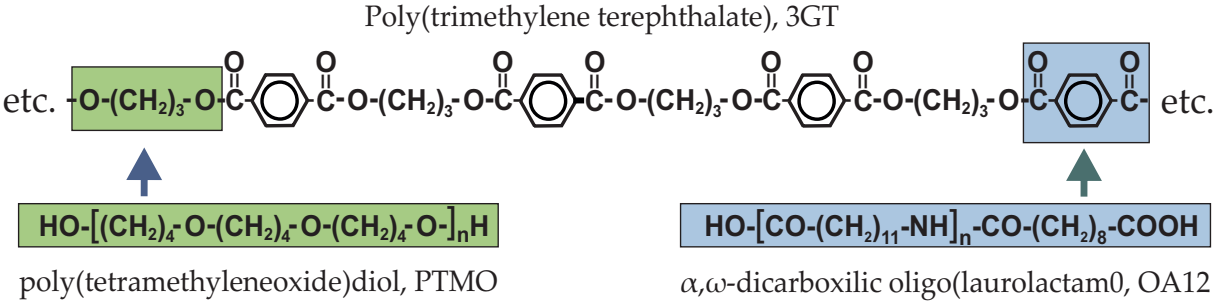

Fig. 1. Modification scheme of poly(trimethylene terephthalate) macromolecule

T a b l e 1. Composition of TPEEA with varied DP_{3GT} and constant OA12 and PTMO

Sample	M_{3GT} g/mol	DP_{3GT}	m_{PTMO}	m_{OA12}	m_{DMT}	m_{3G}	w_{PTMO}	w_{3GT}	w_{OA12}
1	206	1	3	1	3	6	0.554	0.076	0.370
2	410	2			5	9	0.515	0.141	0.343
3	720	3.5			8	15	0.466	0.224	0.310
4	930	4.5			10	18	0.438	0.270	0.292
5	1130	5.5			12	23	0.413	0.312	0.275
6	1440	7			15	28	0.381	0.366	0.254

M_{3GT} – molecular weight of the ester block, DP_{3GT} – degree of polymerization of the ester block, m – molar ratio, w – weight fraction

ity of 3.6 dm^3, made of acid-resistant steel, equipped with a cooler, heating system, vacuum system and ribbon mixer. The synthesis of terpoly(ester-b-ether-b-amides) (TPEEA) s was conducted in two stages. The first stage involved the transesterification of DMT with 3G (185°C, 90% yield) and the esterification (in a separate reactor) of OA12 with PTMO (230°C, 90% yield) in the presence of a catalyst. The second stage of the process was condensation polymerization of the mixed intermediate products obtained in the first stage of synthesis (255°C; 0.4 mPa, 3 h) [42].

The synthesis of block terpolymers involved the modification of the macromolecule poly(trimethylene terephthalate) (3GT). As a result of this modification, certain sequences derived from terephthalic acid were replaced with the OA12 block, and those derived from 3G were replaced with the PTMO block (Fig. 1).

As a result of the conducted syntheses, a series of TPEEA was obtained, consisting of a rigid amide block OA12 with a molecular weight of 2000 g/mol, a flexible ether block PTMO with a molecular weight of 1000 g/mol, and an ester block 3GT serving as a compatibilizer for the other two blocks. The variable in this series was the degree of polymerization of the 3GT block. The composition of the obtained polymers, as well as the weight and molar ratios of individual blocks, are presented in Table 1.

Methods

To characterize the basic physicochemical properties of the obtained TPEEA, the following measurements were conducted: intrinsic viscosity (30°C, phenol-trichloroethylene 50/50 w/w, capillary I), water and benzene absorption (20°C, 72 h) and hardness in Shore A and D scales, 20°C (type 3100 instrument, ZwickRoell, Ulm, Germany) according to ISO 868 standard.

Thermal properties were examined using DSC with heating-cooling-heating cycle at a rate of 10°C/min (Q100, TA Instruments, New Castle, USA) and DMTA with heating rate of 1°C/min, 1 Hz (Q800, TA Instruments, New Castle, USA).

Phase distribution of synthesized TPEEA was characterized using WAXS (Philips, *X'*Pert PRO MPD diffractometer, Amsterdam, The Netherlands) with a wide-angle goniometer with CuKα radiation with a wavelength of 1.54 Å (monochromatized with nickel).

The chemical structure of macromolecules was investigated using FTIR spectroscopy (Thermo Nicolet, 32 scans, resolution 2 cm^{-1}, wavenumber range 400–4000 cm^{-1}).

Mechanical properties, including mechanical hysteresis loops, were determined during static tension (Instron, type 5982, Norwood, MA, USA) at a speed of 100 mm/min and a load of 10 kN at 20°C.

Sample preparation

Granulated and vacuum-dried terpolymers were processed into specimens for determining hardness, dynamic, static, and elastic mechanical properties (paddle-shaped) and for WAXS and FTIR tests (disc-shaped). Paddles with a length of 50 mm and a cross-sectional area of 12 mm^2 were obtained by injection molding method (injection temperature set 10°C higher than the polymer melting point determined optically). Circular discs with a diameter of 25 mm and a thickness of 0.5 mm were formed using compression molding at a temperature 20°C higher than the polymer melting point determined optically. The compression pressure applied was 20 MPa.

RESULTS AND DISCUSSION

Chemical structure of TPEEA

The TPEEA spectra exhibit all characteristic bands for esters, ethers, and amides (Fig. 2): 3293 cm^{-1} – stretching vibrations of N-H groups involved in hydrogen bonding, stretching vibrations of O-H in end groups, 3090 cm^{-1} – Fermi resonance of N-H groups, 2918 cm^{-1} – asymmetric stretching vibrations of C-H groups in CH_2 groups, 2848 cm^{-1} – symmetric stretching vibrations of C-H groups in CH_2 groups, 1715 cm^{-1} – stretching vibrations of the carbonyl group C=O in the ester bond, 1635 cm^{-1} – I amide band, 1557 cm^{-1} – II amide band, 1465 cm^{-1} – bending vibrations of CH_2 groups adjacent to the N-H group, 1408 cm^{-1} – stretching vibrations of C=C in the aromatic ring, 1366 cm^{-1} – deformation vibrations of O-H groups, 1268 cm^{-1} – asymmetric stretching vibrations of Ar-C-OO-C groups and overlapped vibrations of the III amide band, 1204 cm^{-1} – stretching vibrations of O-H groups, 1099 cm^{-1} – symmetric stretching vibrations of C-O-C groups in the

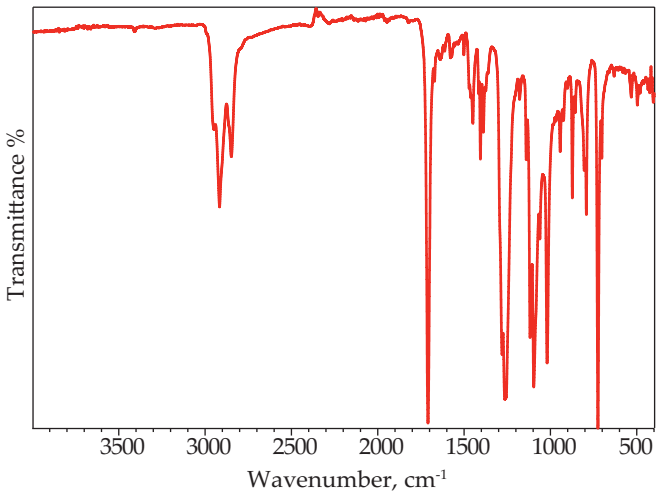

Fig. 2. FT-IR spectra of TPEEA with DP_{3GT} = 3.5

ester and ether blocks, 1019 cm^{-1} – in-plane stretching vibrations of C-H groups in the aromatic ring, 875 cm^{-1} – rocking vibrations of CH_2 groups in -O-$(CH_2)_n$-O- groups, 729 cm^{-1} – out-of-plane bending vibrations of C-H groups in the aromatic ring, 519 cm^{-1} – IV amide band.

To confirm the incorporation of amide and ester blocks into the 3GT macromolecule structure, spectra of the obtained terpolymers were compared with homopolymers PTMO and OA12 (Fig. 3). In the TPEEA spectrum, there is no broad, diffuse absorption band at a wavelength of 3440 cm^{-1} present in the homopolymer PTMO spectrum. Significant reduction in the intensity of signals at wavelengths 1366 and 1204 cm^{-1} is also observed. These bands correspond to the vibrations of hydroxyl end groups in polyether and polyester. The absence or substantial weakening of these signals indicates a reduction in the concentration of end groups, implying the incorporation of the PTMO block into the 3GT macromolecule. Additionally, the TPEEA spectrum lacks the signal at a wavelength of 3291 cm^{-1}, which is present in OA12 and corresponds to the stretching vibrations of O-H in terminal carboxyl groups. This confirms the incorporation of the OA12 block into the 3GT macromolecule.

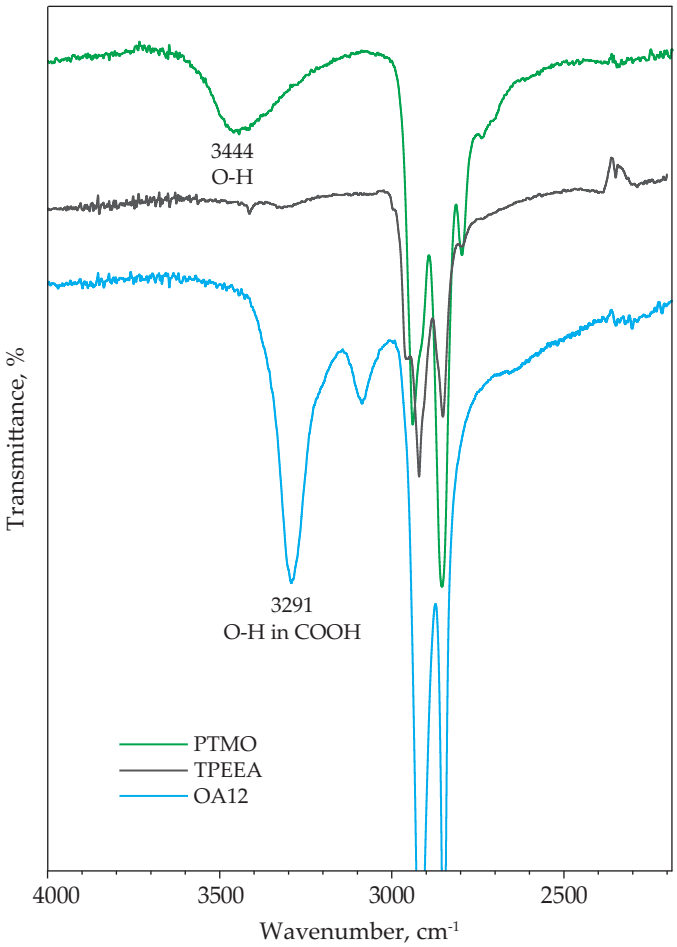

Fig. 3. Comparison of FTIR spectra of TPEEA copolymers (DP_{3GT} = 3.5), PTMO and OA12 homopolymers

With the increase in DP_{3GT}, the intensity of bands corresponding to groups present in the ester block also increases. As a representative example, the band at a wavelength of 1715 cm^{-1} was selected (Fig. 4). A similar effect can be observed for the other bands characteristic of aromatic polyesters (1408, 1268, 1019, 729 cm^{-1}).

The obtained FTIR results confirm that during the first stage of TPEEA synthesis, a series of 3GT blocks with increasing degrees of polymerization was obtained, and

T a b l e 2. Selected properties of TPEEA

DP_{3GT}	η dL/g	H Shore A	H Shore D	p_{H2O} %	p_b %	T_m^p °C	T_m^k °C
1	1.68	83	20	2	180	138	144
2	1.57	79	18	2	182	124	141
3.5	1.77	68	17	5	243	105	124
4.5	1.68	77	17	2	200	107	121
5.5	1.58	76	16	1	149	118	136
7	1.19	75	16	2	137	122	145

η – limiting viscosity number, H – hardness, p_{H2O} i p_b – water and benzene absorption, T_m^p, T_m^k – the beginning and end of the melting point examined optically.

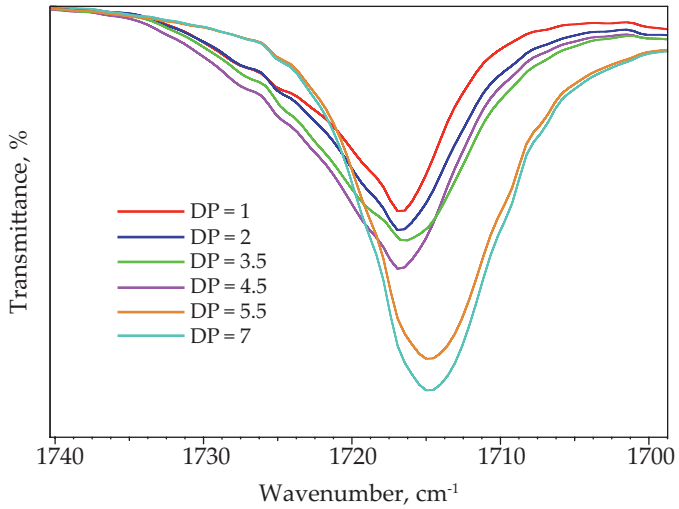

Fig. 4. The effect of DP_{3GT} on the intensity of the adsorption band responsible for the stretching vibrations of the carbonyl group of the ester bond in the 3GT ester block

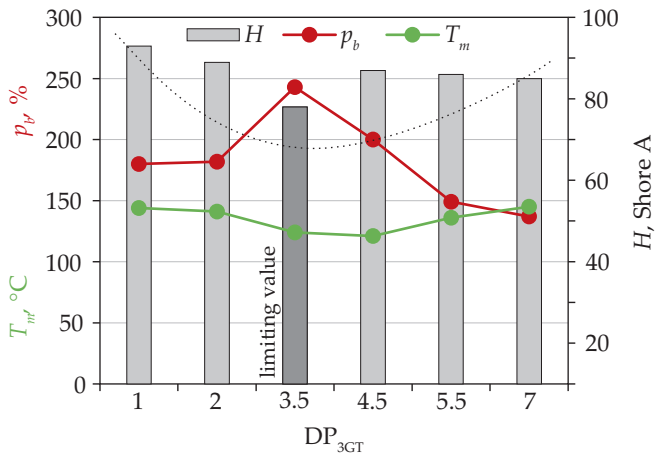

Fig. 5. The effect of DP_{3GT} on selected physical properties

in the second stage, effective modification was carried out according to the scheme presented in Fig. 1.

Selected properties of TPEEA

The main physicochemical properties of the obtained TPEEA are presented in Table 2. The relationship between intrinsic viscosity and polymer molecular weight is described by the Mark-Houwink equation $[\eta] = K \cdot M\alpha$, where the parameters K and α characterize polymer-solvent interactions. Determining these parameters in complex multiblock systems poses numerous challenges. Therefore, it is common to establish a critical value $[\eta_{gr}]$, beyond which terpolymers exhibit good mechanical properties. It is then assumed that at $[\eta]$ values higher than $[\eta_{gr}]$, the polymers have satisfactory molecular weights. For TPEAA, $[\eta_{gr}]$ = 1,25 dL/g [15]. The synthesized materials mostly showed $[\eta]$ values > 1,25 dL/g, indicating that they are composed of macromolecules with sufficiently large molecular weights.

The consequence of the interaction between the solvent and the polymer matrix is its swelling. This results in a change in the spatial geometry of the material, expressing the exchange of enthalpy between the two phases of polymer-solvent. Consequently, it allows for the assessment of the size and quality of the continuous phase in the polymer. An increase in DP_{3GT} leads to an increase in TPEEA's benzene swelling, a decrease in hardness, and a reduction in the melting temperature (Fig. 5). This indicates that a more well-defined polymer matrix is formed, consisting of 3GT blocks. However, it seems that DP_{3GT} = 3.5 is a critical value, beyond which the observed trend reverses.

Thermal properties and phase distribution of TPEEA

Thermal properties and phase structure of the obtained TPEEA were examined using DSC, DMTA, and WAXS methods. Based on these studies, employing the methodology described in [11, 42], the phase composition of TPEEA was determined qualitatively and quantitatively. The assessment of the properties of the obtained TPEAA was preceded by the analysis of individual homopolymers and copolymers built from combinations of blocks constituting the terpolymer. Their Hildebrand solubility parameters were calculated to estimate mutual solubility. These results are extensively described in [42].

On the diffractogram of the 3GT homopolymer, six points of diffracted radiation intensity can be observed at reflection angles 2θ: 15.08°; 16.51°; 19.17°; 23.19°; 24.39°; and 26.91°. The diffractogram of the OA12 homopolymer exhibits a single broad diffraction maximum with two extreme points: 19.75° and 21.75°, resulting from the overlap of reflections from two polymorphic structures, γ and

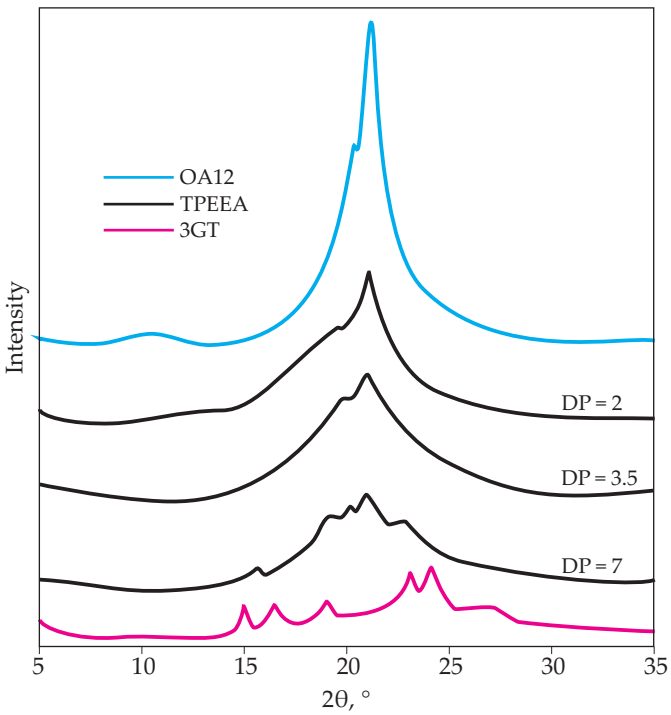

Fig 6. WAXS diffractograms of homopolymers 3GT, OA12 and copolymers TPEEA with varied DP_{3GT}

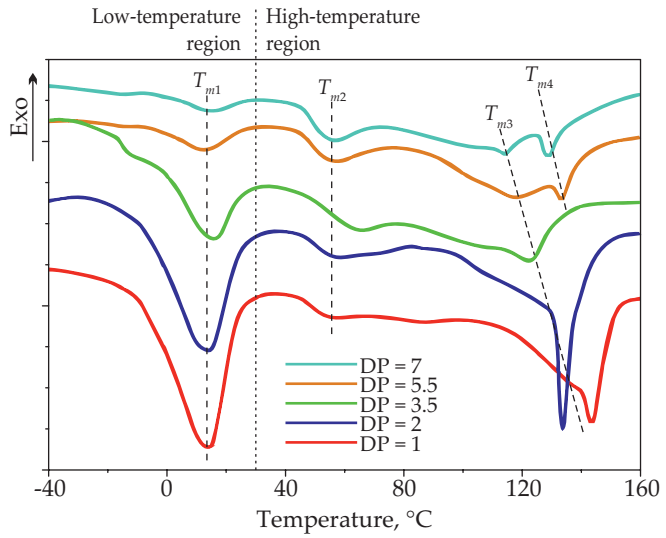

Fig. 7. Second heating DSC thermograms of TPEEA with varied DP_{3GT}

α OA12. In the TPEEA diffractograms, only reflections at 2θ angles corresponding to the values on the OA12 diffractogram are present. Therefore, it can be inferred that in the obtained materials built from rigid 3GT and OA12 blocks, the formation of the crystalline phase is solely attributed to the OA12 block. This rule applies when the weight fraction of ester blocks is less than 0.3. At higher fractions of this block, in addition to the amidic crystalline phase, an additional crystalline phase composed of rigid ester blocks is separated. The diffractograms of these materials differ significantly from the others and are a superposition of the diffractograms of the OA12 and 3GT homopolymers (Fig. 6).

The glass transition temperatures (T_g) were determined from the maximal value of the storage modulus (E'') and the loss angle (tan Delta) (Fig. 8 and 9). Meanwhile, DSC analysis (Fig. 7) allowed the determination of the crystallization temperature (T_c), crystallization enthalpy change (ΔH_c), melting temperature (T_m), and melting enthalpy change (ΔH_m) of individual phases of the copolymer. The temperature range of the study was divided into two regions: low-temperature (<30°C) and high-temperature (>30°C) region. In the low-temperature region, transformations characteristic of the soft phase of TPEEA were observed, while in the high-temperature region, transformations corresponding to the intermediate and hard phases were noted.

The observed glass transition temperature (T_{g1}) in the low-temperature region averages -60°C and is constant for the entire copolymer series, while the T_g of the PTMO homopolymer is -90°C. It is assumed that the stiffening of the ends of the flexible block chain by the chemical bonding of the rigid block raises the glass transition temperature by about 10°C, and interactions between the continuous phase and the dispersed phase can further increase this temperature by another 5°C [1, 53–55]. Therefore, such a significant increase in T_g cannot be explained solely by the mentioned phenomena. The increase in T_g of PTMO is due to the dissolution of short ester sequences in the ether block phase. However, the analysis of the solubility parameter values δ of these blocks indicates that they are mutually immiscible: $(\delta_{PTMO} - \delta_{3GT})^2 = 5{,}9$ MPa. It should be noted, though, that for each polymer mixture, a critical molecular weight of the components can be determined, below which, despite the thermodynamic incompatibility of the components, the system will form a homogeneous mixture [56]. For the 3GT-PTMO system, the critical molecular weight of the ester block is 600 g/mol, so 3GT blocks with $DP_{3GT}<3{,}5$ will at least partially mix with the PTMO block fraction.

With the increase in DP_{3GT}, the thermal effect associated with the melting of PTMO blocks (T_{m1}) diminishes. This is caused by the decreasing volume of the soft phase, which becomes increasingly contaminated with other blocks, leading to a worsening phase separation between the soft and hard phases.

In the high-temperature region, there is an increasing flattening of the endotherm corresponding to the

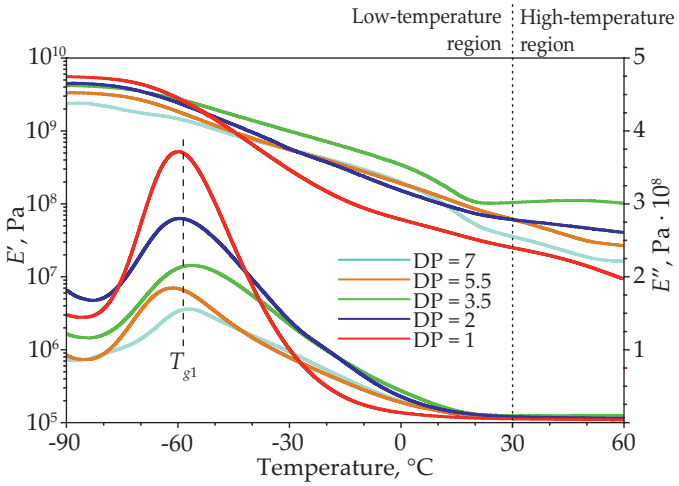

Fig. 8. Dependence of the storage modulus (E') and loss modulus (E'') on temperature for TPEEA with varied DP_{3GT}

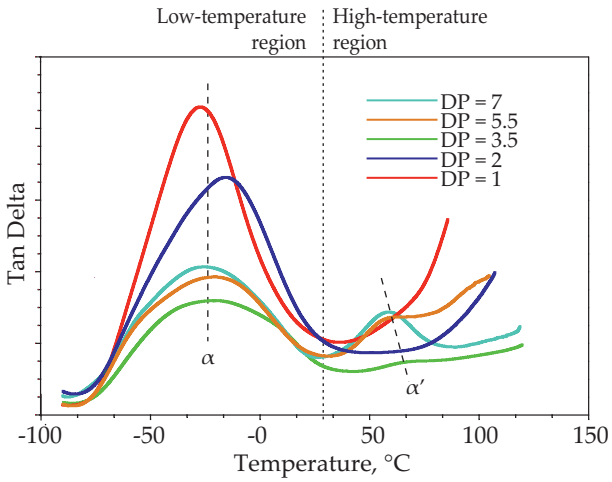

Fig. 9. Values of the maximum loss angle (tan Delta) TPEEA with varied DP_{3GT}

enthalpy ΔH_{m3} and the melting temperature T_{m3} of the crystalline hard phase of the terpolymer. The maximum of this endotherm is also shifting towards lower temperatures. This is caused by the dissolution of short sequences of 3GT in OA12 and the worsening perfection of the amide crystalline phase. This fact is confirmed by the shifting of the crystallization peaks of OA12 towards lower temperatures. At DP>3.5, an additional crystalline phase composed of ester blocks begins to separate (another melting endotherm T_{m4} appears). In the case of both T_{m3} and T_{m4}, there is a phenomenon of lowering the temperature below the melting temperatures of both components, known as the melting temperature depression [11, 56, 57]. This indicates a significant disruption of the crystalline structure of the system, caused by the mutual dissolution of short fragments of 3GT and OA12 blocks.

The temperature spectra of the obtained TPEEA exhibit a typical behavior for thermoplastic elastomers. In the temperature range from -100°C to -70°C, the functions $E' = f(T)$ has a flat profile, their modulus remains constant, and the TPEEA are completely glassy. In the range from -70°C to 0°C, there is a decrease in modulus (macroscopic viscoelastic relaxation processes are activated in the macromolecules). The third temperature range is the "elasticity plateau", where the modulus in this range is constant. The width of this range slightly decreases with an increase in DP_{3GT}. At a temperature about 30°C lower than the T_{m3} determined from DSC, the elastomers exhibit a prevalence of viscous characteristics over elastic ones, and their modulus sharply decreases. Maxima of damping occur at a constant temperature of about -60°C, corresponding to the glass transition processes of the amorphous phase of flexible blocks. No influence of DP_{3GT} on the glass transition temperature is observed. On the tan Delta = $f(T)$ curve of TPEEA obtained with the participation of the 3GT block with $DP_{3GT} \geq 3.5$, an additional relaxation transition, probably associated with the glass transition of the amorphous phase of the 3GT blocks, can be observed.

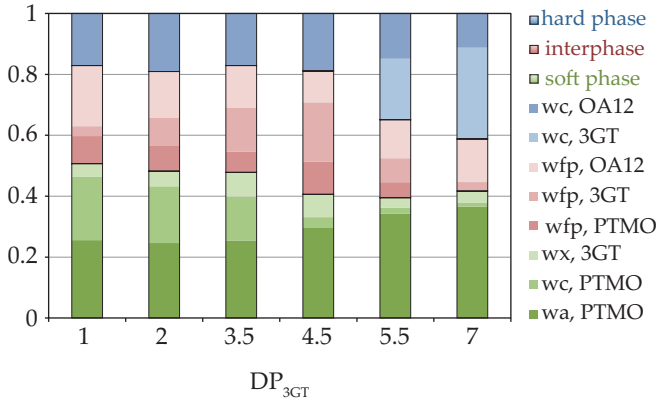

where: wa, PTMO – amorphous fraction of flexible PTMO blocks forming the soft phase; wc, PTMO – crystalline fraction of flexible PTMO blocks forming the soft phase; wx,3GT – short 3GT sequences dissolved in the soft phase; wfp, PTMO – PTMO blocks forming the intermediate phase (interphase); wfp, 3GT – 3GT blocks forming the intermediate phase; wfp, OA12 – OA12 blocks forming the intermediate phase; wc, 3GT – 3GT blocks forming the hard phase; wc, OA12 – OA12 blocks forming the hard phase.

Fig. 10. Phase composition of TPEEA with varied DP_{3GT}

The assessment of the phase composition of copolymers is based on calculations of the degree of separation, the crystallinity degree of the continuous phase, and the crystallinity degree of the dispersed phase. The calculations were performed using the methodology described in [42]. The results are presented in Figure 10.

Analyzing the phase composition of the obtained TPEEA, it can be observed that $DP_{3GT} = 4.5$ seems to be a critical value above which the physical properties of these materials change drastically. TPEEA with $DP_{3GT} \leq 4.5$ exhibit a constant weight fraction of each

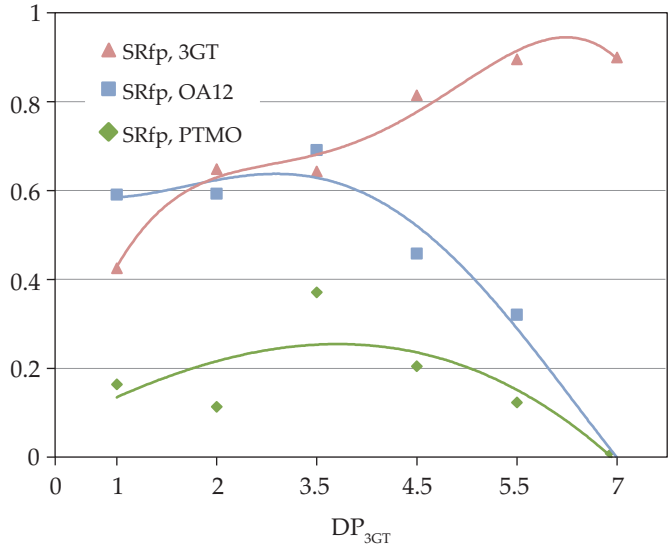

Fig. 11. Dependence of the degree of phase separation of the intermediate phase on DP_{3GT} TPEEA

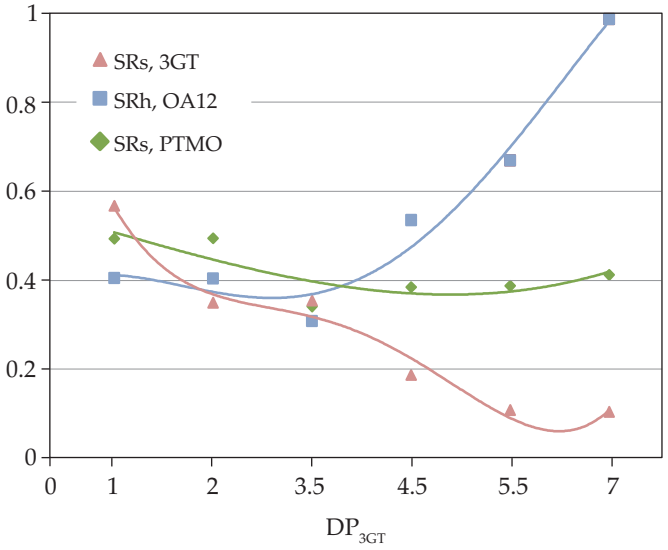

Fig. 12. Dependence of the degree of phase separation of the soft and hard phases on DP_{3GT} TPEEA

T a b l e 3. Mechanical and elastic properties of terpolymers

DP_{3GT}	σ, MPa	ε, %	*E*, MPa	ε_n, %	ε_e, %	ε_s, %	R_{II}, %	R_V, %	A	BII	BV	ΔB, %	C
1	4.4	119	19.2	27.0	1.5	72.7	98.5	100	109	43	28	34	217
2	3.6	200	15.9	24.6	1.4	75.4	98.6	99.8	102	37	25	33	90
3.5	3.0	309	4.2	28.3	0.5	71.6	99.5	100	68	16	11	31	94
4.5	3.2	58	17.4	–	–	–	–	–	–	–	–	–	–
5.5	3.8	47	21.6	–	–	–	–	–	–	–	–	–	–
7	3.5	34	30.7	–	–	–	–	–	–	–	–	–	–

σ – tensile strength, ε – elongation at break, *E* – Young's modulus, ε_n – permanent elongation, ε_e – delayed high-elastic elongation, ε_s – immediate elastic elongation, R_{II} and R_V – elastic recoveries in the second and fifth stretching cycles, A – area proportional to the elastic dispersed energy, B_{II} and B_V – areas proportional to the high-elastic dispersed energy during the second and fifth stretching cycles, ΔB – percentage change in the amount of high-elastic dispersed energy between the second and fifth cycles, C – area proportional to the accumulated energy.

phase, and with an increase in DP_{3GT}, only their qualitative composition changes. In these materials, only the crystallizing OA12 blocks form the hard phase, while the soft phase consists of amorphous and crystalline fractions of PTMO blocks contaminated with a small number of amorphous fractions of 3GT blocks. In TPEEA with $DP_{3GT} \geq 4.5$, an increase in the content of the hard phase at the expense of the intermediate phase is observed. This leads to a better separation of 3GT blocks, resulting in the emergence of a second crystalline phase primarily composed of 3GT blocks. As DP_{3GT} increases, PTMO blocks lose their ability to crystallize. It can be inferred that short ester sequences (below 600 g/mol) act as crystallization nuclei in this system. The composition of the intermediate phase also changes fundamentally, having an ether-amide structure for $DP_{3GT} < 3.5$, an ester-ether-amide structure for $3.5 \leq DP_{3GT} \leq 4.5$ and an ester-amide structure for $DP_{3GT} > 4.5$. Since the composition and size of the intermediate phase determine many characteristics of TPEEA, the proportions of individual blocks in its composition were calculated relative to the proportions of the corresponding blocks in the entire terpolymer and in relation to the intermediate phase. As a criterion for evaluating the portion of a given block within each phase involves the use of separation degrees for blocks forming the soft phase (SRs), hard phase (SRh), and intermediate phase (SRfp). The relationships depicted for the degree of separation of individual blocks in the intermediate phase, as well as the soft and hard phases, indicate that the intermediate phase results from imperfections in the separation of the soft and hard phases. The separation curves of blocks in the intermediate phase (Fig. 11) are a mirror reflection of the separation curves of these blocks in the soft and hard phases (Fig. 12) and create their negative image.

Mechanical properties of TPEEA

Table 3 presents tensile properties, including tensile strength (σ), elongation at break (ε), and Young's modulus (E). Additionally, a series of parameters describing the elastic properties of the materials were determined. The strength tests have confirmed previously drawn

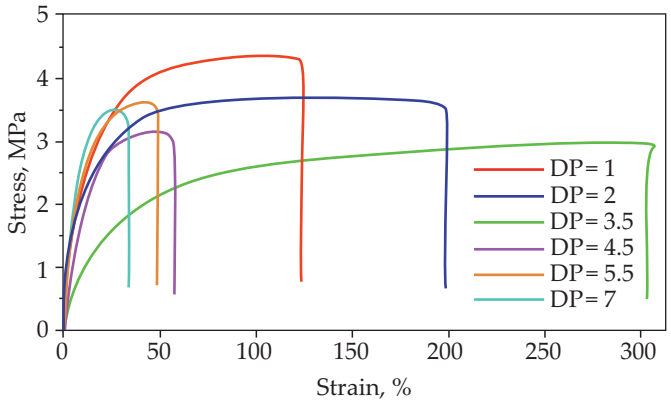

Fig. 13. Stress-strain curves of TPEEA with varied DP_{3GT}

conclusions that $DP_{3GT} \approx 3.5$ is a critical value, beyond which the obtained materials undergo a drastic change in their properties. The stress-strain curves of TPEEA with $DP_{3GT} \leq 3.5$ exhibit characteristics typical for thermoplastic elastomers (Fig. 13), where no yield point is observed. Also, the characteristic upward bending induced by crystallization, typical for natural rubbers, is not observed. With the increase in DP_{3GT}, the elongation at break (ε) of TPEEA increases until reaching a value (about 300%), after which a sharp decrease is observed.

To assess the elastic properties of TPEEA, two types of mechanical hysteresis loops characterizing elasticity and stress relaxation were conducted. The first type was obtained by stretching the samples five times at 100% strain and then releasing the stress (Fig. 14a), while the second type involved stretching the samples from 10% to 100% with incremental 10% elongation (Fig. 14b).

The ability to immediately return after deformation is expressed by the elastic elongation (ε_s) and the area A proportional to the elastic dispersed energy. They are a measure of the quality of the spatial network of the elastomer, capable of transmitting high stresses. High-elastic elongation (ε_e) and the area B proportional to the high-elastic dispersed energy characterize the material's ability to delayed recovery after deformation and are a measure of the quality of the continuous phase capable of exhibiting viscoelastic response. For permanent deformation (ε_n) and the area C proportional to the accumulated energy, they correspond to irreversible changes

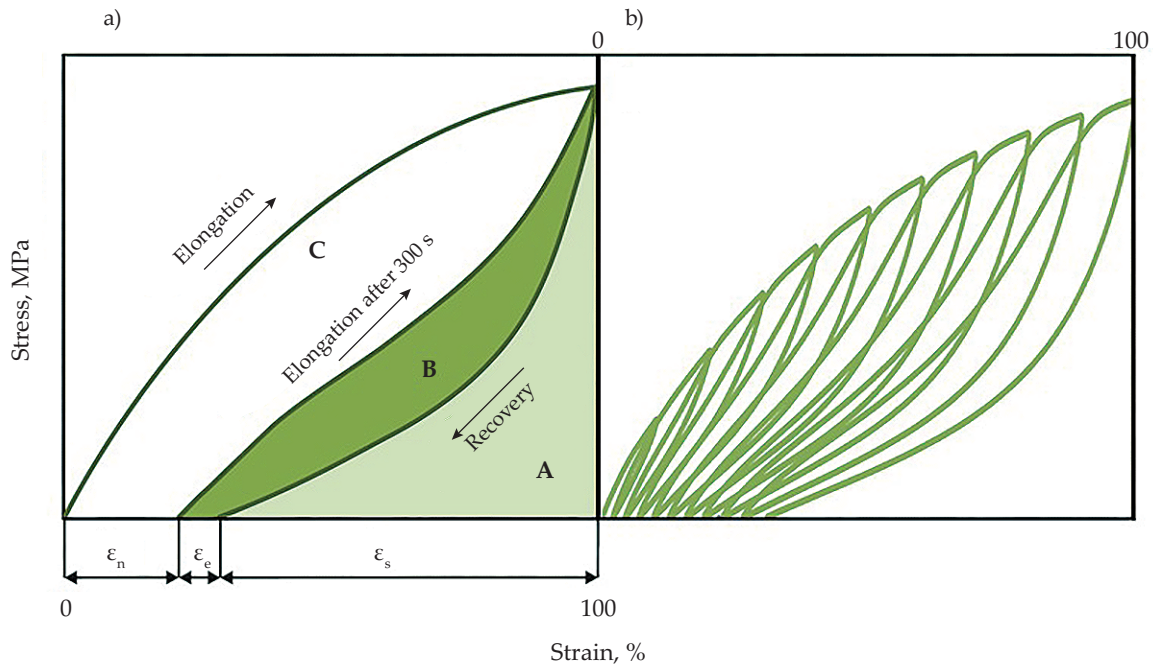

where: ε_n – irreversible (permanent) elongation; ε_e – delayed high-elastic elongation; ε_s – elastic elongation; A – area proportional to the elastic energy dispersed; B – area proportional to the high-elastic energy dispersed; C – area proportional to the energy accumulated.

Fig. 14. Mechanical hysteresis loops: a) at a constant elongation of 100%, b) with increasing 10% elongation

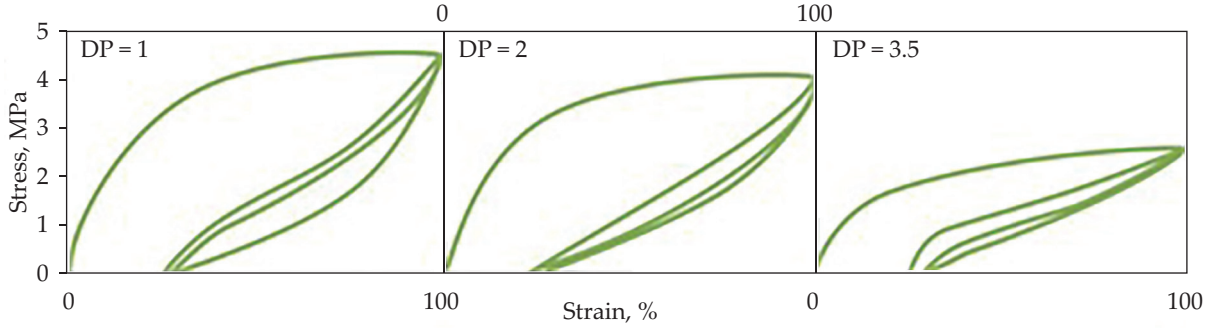

Fig. 15. Mechanical hysteresis loops at a constant elongation of 100% TPEEA with varied DP_{3GT}

that occurred in the material under stress, associated with a change in the spatial distribution of domains (their orientation and reorientation). This assumption is confirmed by the significant energy accumulation in the first cycle and little energy absorption in subsequent cycles. With the increase in DP_{3GT}, the value of the dispersed energy in the first stretching cycle decreases (Fig. 15). A more well-developed elastomeric spatial network capable of transmitting high stresses is formed. The crystalline domains of OA12 are embedded in the matrix, allowing for their free movement and, consequently, returning to the original position after releasing the stretching stress.

The obtained materials in the second and subsequent stretching cycles exhibit elastic recoveries above 98%. However, it should be noted that in the first cycle, they achieve elastic recoveries at only ~75%. This is due to the loss of energy in organizing the spatial structure of the material's internal structure. Such behavior suggests that any products made from TPEEA should undergo preliminary training (mechanical conditioning) before actual use.

CONCLUSIONS

The properties of TPEEA result from the combination of individual characteristics of its component blocks. Therefore, changing their relative mass ratios enables the modification of the overall macromolecule properties in the desired direction. The key to designing TPEEA is to select components in such a way that a stable micro- or nanostructure is formed, depending on interblock, intermolecular and interfacial interactions. The obtained systems are composed of at least three phases: a soft phase,

a hard phase, and an interphase. The soft phase consists of flexible PTMO blocks contaminated with a certain amount of 3GT blocks. The degree of polymerization of the ester block significantly affects the composition of the hard phase. In the case of $DP_{3GT} < 4.5$, the hard phase is primarily composed of rigid OA12 blocks. However, a further increase in DP_{3GT} causes the appearance of a second dispersed crystalline phase consisting of 3GT blocks. Based on this, it can be inferred that only ester blocks with low molecular weights (<600 g/mol) can mix with other blocks, modifying the phases that constitute them and stabilizing the micro- and nanophase structure of the entire system. In the PTMO block phase, short ester sequences act as nucleation precursors, while in the hard OA12 phase, they function as plasticizers.

Author contribution

J.R. – conceptualization, formal analysis, investigation, resources, data curation, writing-original draft preparation, supervision; J.J. – resources, visualization; B.S. – methodology, visualization; K.W. – methodology, data curation, writing-review and editing. All authors have read and agreed to the published version of the manuscript.

Funding

This research received no external funding.

Conflict of interest

The authors declare no conflict of interest.

REFERENCES

[1] Holden G.: "Thermoplastic Elastomers. Encyclopedia of Polymer Science and Technology", John Wiley & Sons, Hoboken 2010, p. 465.

[2] Naskar K., Babu R.R.: "Thermoplastic Elastomers (TPEs) and Thermoplastic Vulcanizates (TPVs)" in "Encyclopedia of Polymeric Nanomaterials" (editor Kobayashi S., Müllen K.), Springer, Berlin 2001, p. 2517. https://doi.org/10.1007/978-3-642-29648-2_310

[3] Aiswarya S., Pratiksha A., Banerjee S.S: *European Polymer Journal* **2022**, *181*, 111658. https://doi.org/10.1016/j.eurpolymj.2022.111658

[4] Holden G.: "Thermoplastic Elastomers" in "Rubber Technology" (editor Morton M.), Springer, Boston 1987, p. 465. https://doi.org/10.1007/978-1-4615-7823-9_16

[5] Drobny J.G.: "Handbook of Thermoplastic Elastomers", William Andrew Inc., Norwich 2014, p. 1.

[6] De S.K., Bhowmick A.K.: "Introduction to Thermoplastic Elastomers" in "Thermoplastic Elastomers from Rubber-Plastic Blends", Ellis Horwood, New York 1990, p. 13.

[7] Rader Ch.R., Abdou-Sabet S.: "Two-Phase Elastomeric Alloys" in" Thermoplastic Elastomers from Rubber-Plastic Blends" (editor De S.K., Bhowmick A.K.), Ellis Horwood, New York 1990, p. 159.

[8] Grady B.P., Cooper S.L., Robertson Ch.G.: "Thermoplastic Elastomers" in "Science and Technology of Rubber" (editor Mark J.E., Erman B., Eirich F.R.), Academic Press, San Diego, New York 2013, p. 591. https://doi.org/10.1016/B978-0-12-394584-6.00013-3

[9] Rzymski W.M., Radush H.J.: *Polimery* **2002**, *47(4)*, 229.

[10] Steube M., Johann T., Barent R.D. *et al*.: *Progress in Polymer Science* **2022**, *124*, 101488. https://doi.org/10.1016/j.progpolymsci.2021.101488

[11] Basu D., Banerjee S.S., Debnath S.Ch. *et al*.: *Polymer* **2023**, *212*, 123309. https://doi.org/10.1016/j.polymer.2020.123309

[12] Mark J.E., Erman B., Roland M.: "The science and technology of rubber", Elsevier Academic Press, Amsterdam, Boston 2013, p. 591. https://doi.org/10.1016/B978-0-12-394584-6.00013-3

[13] McKeen L.W.: "Thermoplastic Elastomers" in "Fatigue and tribological properties of plastics and elastomers", William Andrew, Oxford 2016, p. 245. https://doi.org/10.1016/B978-0-08-096450-8.00010-7

[14] Fakirov S.: "Poly(Ether Ester) Thermoplastic Elatomers: Phase and Deformation Behavior on the Nano- and Microlevel" in "Handbook of Condensation Thermoplastic Elastomers", Wiley-VCH, Weinheim 2005, p. 167. https://doi.org/10.1002/3527606610.ch6

[15] Ukielski R.: *Polymer* **2000**, *41(5)*, 1893. https://doi.org/10.1016/S0032-3861(99)00304-3

[16] Leibler L.: *Macromolecules* **1980**, *13(6)*, 1602. https://doi.org/10.1021/ma60078a047

[17] Desper R.C., Bryne C.A., Li Y. *et al*.: *Macromolecules* **1995**, *28(12)*, 4213. https://doi.org/10.1021/ma00116a024

[18] Koberstein J.T., Russel T.P.: *Macromolecules* **1986**, *19(3)*, 714. https://doi.org/10.1021/ma00157a039

[19] Elwell M.J., Ryan A.J., Gruenbauer H.J.M. *et al*.: *Macromolecules* **1996**, *29(8)*, 2960. https://doi.org/10.1021/ma9511208

[20] van der Schuur M.J., van der Heide E., Feijen J. *et al*.: *Polymer* **2004**, *48(8)*, 2721. https://doi.org/10.1016/j.polymer.2004.02.016

[21] van der Schuur M.J., de Boer J., Gaymans R.J.: *Polymer* **2005**, *46(22)*, 9243. https://doi.org/10.1016/j.polymer.2005.07.041

[22] van der Schuur M.J., Gaymans R.J.: *Journal of Polymer Science Part A: Polymer Chemistry* **2006**, *44(16)*, 4769. https://doi.org/10.1002/pola.21587
[23] Ramon J., Saez V., Gomes F. *et al*.: *Macromolecular Symposia* **2018**, *380(1)*, 1800065. https://doi.org/10.1002/masy.201800065
[24] Xiao R.Z., Zeng, Z.W., Zhou, G.L. *et al*.: *International Journal of Nanomedicine* **2010**, *5*, 1057. https://doi.org/10.2147/IJN.S14912
[25] Nguyen T.H., Petchsuk A., Tangboriboonrat P. *et al*.: *Advanced Materials Research* **2010**, *93–94*, 198. https://doi.org/10.4028/AMR.93-94.198
[26] Wang Y., Wu H., Wang Z. *et al*.: *Polymers* **2019**, *11(6)*, 965. https://doi.org/10.3390/polym11060965
[27] Navarro L., Minari R.J., Vaillard S.E.: *RSC Advances*, **2019**, *9*, 482. https://doi.org/10.1039/C8RA09336A
[28] van der Schuur M., Feijen J., Gaymans R.J.: *Polymer* **2005**, *46(13)*, 4584. https://doi.org/10.1016/j.polymer.2005.02.074
[29] Armstrong S., Freeman B., Hiltner A. *et al*.: *Polymer* **2012**, *53(6)*, 1383. https://doi.org/10.1016/j.polymer.2012.01.037
[30] Szymczyk A., Nastalczyk J., Sablong R.J. *et al*.: *Polymers for Advanced Technologies* **2011**, *22(1)*, 72. https://doi.org/10.1002/pat.1858
[31] Paszkiewicz S., Szymczyk A., Pawlikowska D. *et al*.: *RSC Advances* **2017**, *7*, 41745. https://doi.org/10.1039/C7RA07172H
[32] Sakurai S., Nokuwa S., Morimoto M. *et al*.: *Polymer* **1994**, *35(3)*, 532. https://doi.org/10.1016/0032-3861(94)90507-X
[33] Ercan N., Durmus A.: *Journal of Applied Polymer Science* **2022**, *139(26)*, e52458. https://doi.org/10.1002/app.52458
[34] Bai L., Hong Z., Wang D. *et al*.: *Polymer* **2010**, *51(23)*, 5604. https://doi.org/10.1016/j.polymer.2010.09.038
[35] Jiang J., Tang Q., Pan X. *et al*.: *Polymers* **2021**, *13(16)*, 2645. https://doi.org/10.3390/polym13162645
[36] van Hutten P.F., Walch E., Veeken A.H.M. *et al*.: *Polymer* **1990**, *31(3)*, 524. https://doi.org/10.1016/0032-3861(90)90397-H
[37] Mahallati P., Arefazar A., Naderi G.: *International Polymer Processing* **2010**, *25(2)*, 132. https://doi.org/10.3139/217.2311
[38] Zolali A.M., Heshmati V., Favis B.D.: *Macromolecules* **2017**, *50(1)*, 264. https://doi.org/10.1021/acs.macromol.6b02310
[39] Kucera L.R., Brei M.R., Storey R.F.: *Polymer* **2013**, *54(15)*, 3796. https://doi.org/10.1016/j.polymer.2013.05.041
[40] Rault J., le Huy H.M.: *Journal of Macromolecular Science, Part B* **1996**, *35*, 89. https://doi.org/10.1080/00222349608220376
[41] Rached R., Hoppe S., Jonquieres A. *et al*.: *Journal of Applied Polymer Science* **2006**, *102(3)*, 2818. https://doi.org/10.1002/app.24547
[42] Rokicka J., Wilpiszewska K., Janik J. *et al*.: *Materials* **2021**, *14(24)*, 7720. https://doi.org/10.3390/ma14247720
[43] Scalfani V.F., Turner, C.H., Rupar P.A. *et al*.: *Journal of Chemical Education* **2015**, *92(11)*, 1866. https://doi.org/10.1021/acs.jchemed.5b00375
[44] Tseng Y.C., Darling S.B.: *Polymers* **2010**, *2(4)*, 470. https://doi.org/10.3390/polym2040470
[45] Botiz I., Darling S.B.: *Materials Today* **2010**, *13(5)*, 42. https://doi.org/10.1016/S1369-7021(10)70083-3
[46] Ahn J.H., Zin W.C.: *Macromolecules* **2000**, *33(2)*, 641. https://doi.org/10.1021/ma9912812
[47] Cho J.: *Polymer* **2016**, *97*, 589. https://doi.org/10.1016/j.polymer.2016.05.068
[48] Robbins S.W., Beaucage P.A., Sai H. *et al*.: *Science Advances* **2016**, *2(1)*, e150111. https://doi.org/10.1126/sciadv.1501119
[49] Xu Z., Lin J., Zhang Q. *et al*.: *Polymer Chemistry* **2016**, *7*, 3783. https://doi.org/10.1039/C6PY00535G
[50] Deng Y., Wei J., Sun Z. *et al*.: *Chemical Society Reviews* **2013**, *42*, 4054. https://doi.org/10.1039/C2CS35426H
[51] Li M., Liu Y., Bansil R.: *The Journal of Chemical Physics* **2010**, *133*, 084905. https://doi.org/10.1063/1.3473067
[52] Rokicka J., Ukielski R.: „Synthesis and Properties of Multiblock Terpoly(Ester-Aliphatic-Amide) and Terpoly(Ester-Ether-Amide) Thermoplastic Elastomers with Various Chemical Compositions of Ester Block" in „Thermoplastic Elastomers – Synthesis and Applications" (editor Das Ch.K.), In Tech, London 2014, p. 21. https://doi.org/10.5772/61215
[53] Xie M., Camberlin Y.: *Die Makromolekulare Chemie* **1986**, *187(2)*, 383. https://doi.org/10.1002/macp.1986.021870218
[54] Stevenson J.C., Cooper S.L.: *Macromolecules* **1988**, *21(5)*, 1309. https://doi.org/10.1021/ma00183a022
[55] Bornschlegl E., Goldbach G., Meyer K.: "Structure and properties of segmented polyamides" in "Frontiers in Polymer Science. Progress in Colloid and Polymer Science" (Editor Wilke E.), Springer Heidelberg, Berlin 1985, p. 119. https://doi.org/10.1007/BFb0114023
[56] van Krevelen D.W., te Nijehuis K.: "Properties of Polymers", Elsevier, Amsterdam 2009, p. 129.
[57] Ukielski R.: *Polimery* **1996**, *41*, 286.

Received 23 XI 2023.
Accepted 11 XII 2023.